arXiv:1704.07545v1 [cond-mat.mtrl-sci] 25 Apr 2017

Electron Transport from Quantum Kinetic Monte Carlo Simulations

Fei Lin[1,3], Jianqiu Huang[1], and Celine Hin[1,2]
[1]*Department of Mechanical Engineering, Virginia Tech, Blacksburg, Virginia 24061 USA*
[1]*Department of Materials Science and Engineering, Virginia Tech, Blacksburg, Virginia 24061 USA and*
[3]*Department of Physics, Virginia Tech, Blacksburg, Virginia, 24061 USA*
(Dated: April 26, 2017)

An exact Quantum Kinetic Monte Carlo method is proposed to calculate electron transport for 1D Fermi Hubbard model. The method is directly formulated in real time and can be applied to extract time dependent dynamics of general interacting Fermion models in 1D. When coupled with Density Functional Theory and Maximally Localized Wannier Functions, our method can be used to predict electron transport in materials in presence of interfaces. The first application of our method on case study of α-quartz dielectric breakdown seems promising.

PACS numbers: 05.10.Ln, 72.20.-i, 05.60.Gg

Introduction. – Understanding electron transport from microscopic simulations is a subject of intensive ongoing researches [1, 2]. Interest in such calculations has grown when a large electric field is applied to semiconducting nano-devices, which eventually leads to dielectric breakdown of semiconducting materials [3–6]. Two important issues arise in such researches: how can one accurately calculate the electrical conductivity in nano-scale devices, and how can one model the dielectric breakdown in these simulations. One popular approach adopts Boltzmann equation description of electron transport [3]. However, exact solution of the Boltzmann equation remains a great challenge and the method is limited to mesoscopic scale devices.

Kinetic Monte Carlo (KMC) was originally designed for studying vacancy diffusion in alloys [7]. The first application of KMC to classical solid state systems was proposed by Bortz et al. in 1975 [8] for the classical Ising model to speed up the simulation near the classical phase transition where conventional Monte Carlo (MC) method suffers from the critical slowing down. A great progress in simulating dynamics of physical systems has been made when KMC was applied to study electron transport using phenomenological transition probabilities [9]. However, few progress in KMC algorithm has been made to explore electron transport of quantum systems from the microscopic lattice scale.

In this Letter, we describe a new modeling approach to address these two questions. We propose a Quantum Kinetic Monte Carlo (QKMC) simulation based on a 1D Fermi Hubbard model in real-time dynamics as opposed to the usual imaginary-time QMC simulation [10–13] of the quantum Hamiltonian. These time dependent simulations enable us to extract the electrical conductivity directly from the real-time evolution of the Fermi Hubbard model. We then relate, using Density Functional Theory (DFT) [14] coupled with Maximally Localized Wannier Function (MLWF) approach [15, 16], the electrical conductivity results to a semiconducting material α-quartz (S_iO_2) in an effort to investigate the dielectric breakdown from purely electronic origin in the microscopic lattice scale.

Model. – We study the following 1D Fermi Hubbard model:

$$\mathcal{H} = -t \sum_{i=1,\sigma=\uparrow\downarrow}^{M} (c^{\dagger}_{i,\sigma} c_{i+1,\sigma} + h.c.) + U \sum_i n_{i\uparrow} n_{i\downarrow} - \sum_i \mu_i n_i, \tag{1}$$

where $c^{\dagger}_{i,\sigma}(c_{i,\sigma})$ is electron creation (annihilation) operator on site i with spin σ, $n_{i,\sigma} = c^{\dagger}_{i,\sigma} c_{i,\sigma}$ is electron density operator with spin σ, t is hopping integral between nearest neighbors, and U is on-site Coulomb interaction. The system has M sites with open boundary condition (OBC). Our hopping integral t will be extracted from DFT coupled with MLWF calculations to be discussed in the next section.

To model the electric field, we apply the above Hamiltonian to an interface system, where on the left side, M_L lattice sites have a chemical potential $\mu = \mu_L$ and on the right side, M_R lattice sites have a chemical potential $\mu = \mu_R$. Such a potential difference between left and right sides ($\mu_L < \mu_R$) will drive electron transport from left to right across the interface as shown in Figure 1.

Due to the electric field, the hopping integral t along z-axis direction is dominant in determining the electrical conductivity of the material, making our 3D material an effective 1D system. Of course, higher dimension will introduce additional hopping terms to the model. Such higher dimensional hopping effect will be addressed in a future paper.

Method. – In this section, we first describe the QKMC method that we developed for the 1D Fermi Hubbard model. We further show that the method can be used to calculate the electric conductivity of the Hubbard model by applying an electric potential difference across the system.

Following the Stochastic Series Expansion (SSE) method [17], we write the partition function of the above

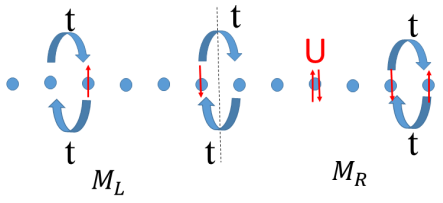

FIG. 1: (Color online.) Schematic picture for 1D system setup. M_L and M_R are the number of lattice sites on the left and right sides of the system. The dashed line represent interface between these two regions. Hopping integral t is between nearest neighbors. Each site can be empty, singly occupied by a spin-up (red up arrow) or -down (red down arrow) electron, or doubly occupied by two electrons, in which case an on-site Coulomb interaction U is introduced to the system.

Hamiltonian as

$$\mathcal{Z} = Tre^{-\beta \sum_{b=1}^{M_b} \mathcal{H}_b}, \tag{2}$$

where $\beta = 1/T$ is inverse temperature, M_b is the number of bonds in the system, and the Hamiltonian Eq.(1) has been written as a summation over bond operators $\mathcal{H}_b$, which is given by

$$\mathcal{H}_b = \begin{cases} \tilde{U} n_{i\uparrow} n_{i\downarrow} - \tilde{\mu}_i n_i & \text{if b is diagonal} \\ -t(c^\dagger_{i\sigma} c_{i+1\sigma} + h.c.) & \text{if b is off-diagonal} \end{cases} \tag{3}$$

Here $\tilde{U} = U/z$ and $\tilde{\mu}_i = \mu/z$ with $z = 2$ the coordination number in 1D.

A series expansion of the partition function to order N_c, which is large enough to contain all expansion terms for temperature T, is carried out. The resulting Hilbert space represented by the series expansion is then sampled by QKMC method. The probability for all possible updates from the present state is tabulated. One typical probability table includes both diagonal and off-diagonal updates. A diagonal update can change the SSE expansion order; while an off-diagonal update changes both the operator type and the states in the series expansion.

It is worth noting that Fermi statistics may introduce a negative sign to the MC weight when a creation (annihilation) operator is applied to a state. However, one can show that in a 1D tight-binding model with OBC such negative signs always appear in pairs, leading to an absence of sign problem for our model (See Supplementary Materials). Ergodicity of the MC simulation is also guaranteed by the combination of diagonal and off-diagonal updates. For details of transition probabilities in QKMC methods, see Supplementary Materials.

An update is picked from the probability table using the standard KMC procedure [8] by uniformly drawing a random number R in the range $[0, Q_K)$. The i^{th} update is chosen if $Q_{i-1} \leq R < Q_i$, where $Q_0 = 0$ and

$$Q_i = \sum_{j=1}^{i} d_j P_j; \;\; i = 1, 2, \cdots, K. \tag{4}$$

Here d_j and P_j are the degeneracy and probability for the j^{th} transition. K is the total number of possible transitions in the system. Once the i^{th} transition is chosen, a second random number $R^{'}$ is drawn uniformly in the range $(0, 1)$. The time interval between the $(i-1)^{th}$ and i^{th} transition is then given by

$$\Delta\tau_i = -(\tau_0/Q_K) \ln R^{'}, \tag{5}$$

where τ_0 is a characteristic time constant determined by the physical model. The cumulative time τ is then proportional to real time in the quantum system evolution.

To access the electrical conductivity, we first equilibrate our system using the above QKMC procedure. A potential difference ($\mu_L < \mu_R$) is then created across the interface to mimic the effects of an applied electric field, which drives the electron transport from the left to the right side of the system. We can, therefore, measure the time evolution of total electron numbers on the right side $N_R(\tau)$, where τ is the cumulative time. The electric current I across the interface is then given by

$$I = e\frac{dN_R}{d\tau}, \tag{6}$$

where e denotes the electron charge. To guarantee that the increase of N_R comes from the decrease of N_L, i.e., from the left side of the system and not from the environment, the above QKMC simulation has to be performed in a canonical system, where $N_R + N_L$ is a constant. We emphasize that μ_L and μ_R in our model Eq.(1) do not refer to a grand canonical system in QKMC simulation. They merely create a potential difference across the interface.

To apply our model Hamiltonian to a real material, we develop the following scheme to extract the effective hopping integral. The energy bands of α quartz are first calculated by VASP software package [18], which shows an energy gap of ~ 9 eV (See Supplementary Materials). An electric field is then applied to the DFT calculations to excite electrons out of the valence bands. Depending on the field strength, different number of bands will be involved in the Wannierization process [15, 16], which is performed with Wannier90 software package [19]. This is reflected in different values of hopping integrals from dif-

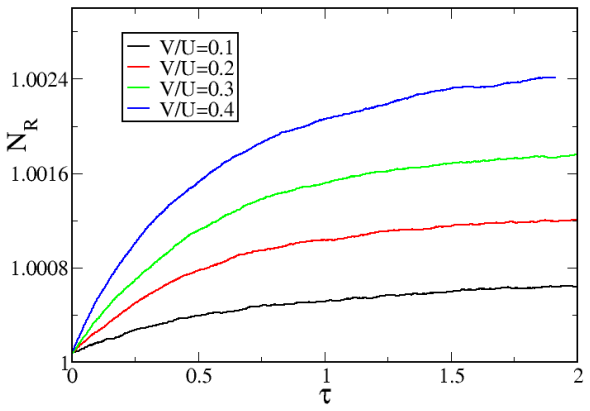

FIG. 2: (Color online.) Average electron number on the right side of the system N_R as a function of KQMC evolution time τ for different applied electric potential difference V across the interface. The system is at half filling, i.e., average 1 electron per site for the whole system. $t/U = 0.5$, and $T/U = 0.1$.

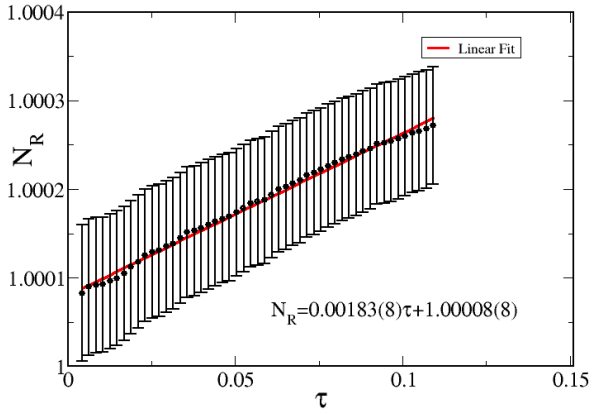

FIG. 3: (Color online.) Transient evolution (black circle) of the average electron number on the right side of the system N_R for $t/U = 0.5$, $V/U = 0.2$, and $T/U = 0.1$. Red straight line is a fit to the transient behavior. Number inside bracket denotes error bar of the fitted coefficient.

ferent electric fields. We will follow the usual practice of evaluating hopping integrals using MLWF as developed by Marzari *et al.*[15, 16].

Numerical results. – We apply the new QKMC simulation algorithm to the Fermi Hubbard model to illustrate our method of electrical conductivity calculation. We set on-site Coulomb interaction $U = 1$ as energy unit.

There are 20 lattice sites with $M_L = 10$ and $M_R = 10$ in our 1D system, which starts with a random configuration and is driven to thermal equilibrium through a typical 10^7 QKMC steps. Here one QKMC step involves the tabulation of probabilities (P_i's) for all possible transitions ($i = 1, \cdots, K$) from the current state, drawing two random numbers, and the subsequent state update. The equilibrium state is then used to generate 10^4 equilibrium configurations, each being separated by 2000 QKMC steps. As a response of these equilibrium configurations to a series of electric potential differences V, where $V = \mu_R - \mu_L$, particle number fluctuations N_R and N_L are recorded as a function of time τ. In Figure 2, we show such evolution, which is averaged over the above 10^4 equilibrium configurations.

To extract the electric current, we focus on the transient and non-equilibrium bahavior of N_R, i.e., in a short evolution time after V is applied. In our method, we shall not look at the long evolution time limit, since such a limit will produce a new equilibrated state of the system, leading to an absence of electron transport across the interface. Figure 3 shows such transient behavior of N_R. A linear fit to the transient data is performed, which yields a transient current $I/e = 0.00183(8)$.

Similar analysis as in Figure 3 can be performed to obtain current I for various potential difference V. The results can be plotted in the current vs. voltage graph (IV curve), as shown in Figure 4. From the Figure 4, we observe a linear behavior of IV curve for small to intermediate V, suggesting an Ohm's law behavior. A linear fit of the IV curve yields slope of the curve as the electric conductivity value of $\sigma = 0.00978(8)$ for $t/U = 0.5$

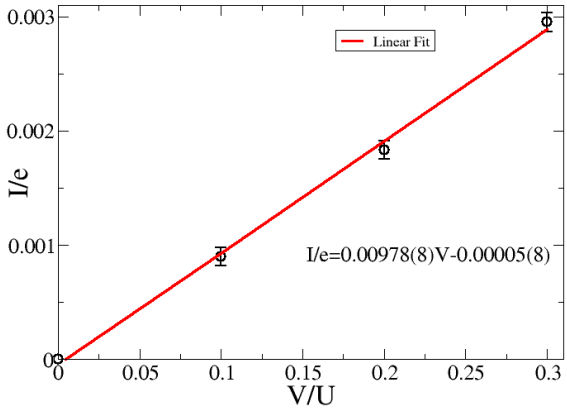

FIG. 4: (Color online.) Transient electric current I/e (black circle) across the interface as a function of potential difference V/U across the interface for $t/U = 0.5$ and $T/U = 0.1$. Red straight line is a linear fit to the IV curve. Number inside bracket denotes error bar of the fitted coefficient.

We further vary the hopping integral t/U in the range

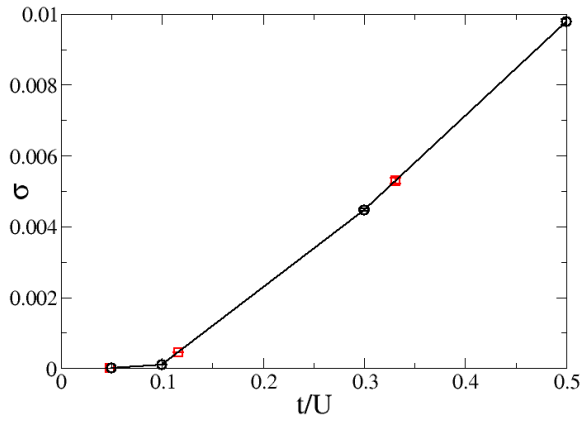

FIG. 5: (Color online.) Electric conductivity σ as a function of hopping integral t for a 20 site system at temperature $T/U = 0.1$. Red squares are electric conductivity for α quartz obtained by assuming $U = 1$ eV in the material.

$[0.05, 0.5]$ and repeat previous analysis. The resulting electric conductivity σ as a function of t/U is plotted in Figure 5, which clearly exhibits a non-linear behavior. At temperature $T/U = 0.1$ we identify the onset of non-zero electric current around $t/U = 0.1$, signaling a gap in the insulating system [20–22].

Based on DFT band structure of α quartz calculated from VASP software package (see Supplementary Materials) [18], we apply the Wannier90 package [19] to obtain the MLWFs and the associated hopping integrals t among MLWFs. See Supplementary Materials. Assuming an on-site Coulomb interaction $U \sim 1$ eV, we can interpolate the electric conductivity values for doped holes in α quartz from Figure 5 and overlay the data in the same graph with red squares. As one can see, the electric conductivity follows a non-linear curve as hopping integral t increases. For $t/U \sim 0.1$, which corresponds to a 2.5 eV electric potential difference (Supplementary Materials), the onset of non-zero conductivity suggests the dielectric breakdown of α quartz from an insulating to a conducting state. Further increase of electric potential will drive the increase of conductivity along a non-linear and non-Ohmic curve.

Discussion – Exact calculation of electron transport is one of the most difficult problems in Condensed Matter Physics. Because of the important role it plays in electric device research, a broad research interest exists in QMC community in developing a feasible method for electric transport. However, the electric transport is essentially a real-time dynamics, which is in sharp contrast to the imaginary-time dynamics inherent in path-integral formulation of the usual QMC methods. Methods based on non-equilibrium Green's function formulation have been proposed [23–26]. Some of the methods are perturbative in nature, while the others are tailored to a specific model. The QKMC method we propose in this Letter can be applied to general Fermion model by performing simulations directly in real time.

QKMC simulation in this Letter is applied to 1D Fermi Hubbard model with OBC, where the notorious sign problem is absent. Extension to higher dimension Fermion models is currently underway and severity of the sign problem will be tested. Compared with the conventional QMC simulations, which can be easily parallelized to increase simulation efficiency, the present QKMC simulation can only be realized in a serial fashion. However, since the electric current calculation starts from an equilibrated state, the conventional QMC can be employed to achieve a faster generation of equilibrated states. The state can then be fed to QKMC for transport calculation. We will explore this possibility together with others in the future.

MLWF analysis of hopping integrals [28, 29] is a key step in connecting our model-based QKMC simulations to real materials. The robustness of 1D results as compared to 2D or 3D systems can be evaluated using essentially the same approach as dicussed in this Letter and the accompanying Supplementary Materials. We expect that electron dynamics is mainly determined by hopping integrals along electric field direction.

Our purely electronic mechanism for dielectric breakdown in this Letter is general and can be applied to various materials, including metal/oxide interface [30, 31], defective interface [32, 33], and amorphous [34] systems. The increase of hopping integral as electric field increases is also general, but the exact hopping integral value will differ for various atomic configuation of materials.

Of course, the mechanism for dielectric breakdown of semiconducting devices might not be just electronic [5, 9]. Effects of other factors, e.g., phonon [35] or defects [36], on electric transport property remain to be determined. Multi-scale modeling of electric transport is still a challenging problem in Condensed Matter Physics. However, our current results point out that purely electronic Fermi Hubbard model captures most of the physics of dielectric breakdown by showing a transition from insulating (zero conductivity) to conducting (finite conductivity) state around $t/U = 0.1$ or with an applied potential difference of 2.5 eV across a unit cell ($6\mathring{A}$). The critical electric field strength is estimated to be 4×10^9 V/m, comparable to 3×10^9 V/m found in experiment [37]. Our new approach agrees well with experiments. Consequently, we can predict accurately and quantitatively the dielectric breakdown in nano-devices within a 1D Fermi Hubbard model approximation.

Summary. – In this Letter we proposed a new and powerful QKMC simulation method for predicting dynamical properties of Fermi Hubbard model. The method can calculate electric conductivity based on the real-time

evolution of the quantum system. The onset of non-zero electric conductivity at low temperatures as hopping integral is increased also manifests the dielectric breakdown of gapped electronic structure to a conducting state for a finite Fermionic system in 1D. When coupled with DFT and MLWF methods, our QKMC algorithm can be employed to predict electron transport property of real materials. Electric conductivity behavior in strong electric field for α quartz, as an application example, seems to be consistent with the dielectric breakdown found in such materials [37].

Acknowledgements – This work was funded by the Air Force with program name: Aerospace Materials for Extreme Environment and Grant No.: FA9550-14-1-0157. We acknowledge Advanced Research Computing at Virginia Tech for providing the necessary computational resources and technical support that have contributed to this work (http://www.arc.vt.edu).

[1] S. Datta, *Quantum Transport: Atom to Transistor*, Cambridge University Press (2005).
[2] M. Luisier, Chem. Soc. Rev. **43**, 4357 (2014).
[3] C. Jacoboni and L. Reggiani, Rev. Mod. Phys. **55**, 645 (1983).
[4] S. Ray, *An Introduction to High Voltage Engineering*, Prentice-Hall of India Private Limited, New Delhi (2004).
[5] F. Chiu, Advances in Materials Science and Engineering **2014**, 578168 (2014).
[6] M. Luisier and A. Schenk, IEEE Trans. on Elec. Dev. **55**, 1494 (2008).
[7] W. M. Young and E. W. Elcock, Proc. of the Phys. Soc. **89**, 735 (1966).
[8] A. B. Bortz, M. H. Kalos, and J. L. Lebowitz, J. Comput. Phys. **17**, 10 (1975).
[9] G. C. Jegert, *Modeling of Leakage Currents in High-κ Dielectrics*, PhD Thesis (2011).
[10] D. M. Ceperley, Rev. Mod. Phys. **67**, 279 (1995).
[11] R. M. Martin, L. Reining, and D. M. Ceperley, *Interacting Electrons, Theory and Computational Approaches*, Cambridge University Press (2016).
[12] J. E. Hirsch, Phys. Rev. Lett. **51**, 1900 (1983).
[13] A. W. Sandvik, J. Phys. A: Math. Gen. **25**, 3667 (1992).
[14] R. M. Martin, *Electronic Structure: Basic Theory and Practical Methods*, Cambridge University Press (2008).
[15] N. Marzari and D. Vanderbilt, Phys. Rev. B **56**, 12847 (1997).
[16] I. Souza, M. Marzari, and D. Vanderbilt, Phys. Rev. B **65**, 035109 (2001).
[17] O. F. Syljuasen and A. W. Sandvik, Phys. Rev. E **66**, 046701 (2002).
[18] G. Kresse and J. Furthmller, Comput. Mat. Sci. **6**, 15 (1996); ibid, Phys. Rev. B **54**, 11169 (1996).
[19] A. A. Mostofi, J. R. Yates, G. Pizzi, Y. S. Lee, I. Souza, D. Vanderbilt and N. Marzari, Comput. Phys. Commun. **185**, 2309 (2014).
[20] G. Kotliar, S. Y. Savrasov, G. Palsson, and G. Biroli, Phys. Rev. Lett. **87**, 186401 (2001).
[21] T. Schafer, F. Geles, D. Rost, G. Rohringer, E. Arrigoni, K. Held, N. Blumer, M. Aichhorn, and A. Toschi, Phys. Rev. B **91**, 125109 (2015).
[22] J. Neumayer, E. Arrigoni, M. Aichhorn, and W. von der Linden, Phys. Rev. B **92**, 125149 (2015).
[23] J. E. Han and R. J. Heary, Phys. Rev. Lett. **99**, 236808 (2007).
[24] T. L. Schmidt, P. Werner, L. Muhlbacher, and A. Komnik, Phys. Rev. B **78**, 235110 (2008).
[25] L. Muhlbacher and E. Rabani, Phys. Rev. Lett. **100**, 176403 (2008).
[26] M. Schiro and M. Fabrizio, Phys. Rev. B **79**, 153302 (2009).
[27] P. Werner, T. Oka, ans A. J. Millis, Phys. Rev. B **79**, 035320 (2009).
[28] S. Zhou and D. M. Ceperley, Phys. Rev. A **81**, 013402 (2010).
[29] R. Kovacik and C. Ederer, Phys. Rev. B **81**, 245108 (2010).
[30] J. Huang, E. Tea, G. Li, and C. Hin, Appl. Sur. Sci. **406**, 128 (2017).
[31] E. Tea, J. Huang, G. Li, and C. Hin, J. Chem. Phys. **146**, 124706 (2017).
[32] E. Tea, J. Huang, and C. Hin, J. Phys. D: Appl. Phys. **49**, 095304 (2016).
[33] G. Li, E. Tea, J. Huang, and C. Hin, arXiv:1611.03411 (2016).
[34] J. Huang, F. Lin, and C. Hin, arXiv:1704.06978 (2017).
[35] J. J. O'Dwyer, Proc. Phys. Soc. B **70**, 761 (1957).
[36] S. Lombardo, J. Appl. Phys.**98**, 121301 (2005).
[37] E. Harari, J. Appl. Phys. **49**, 2478 (1978).

SUPPLEMENTARY MATERIALS FOR "ELECTRON TRANSPORT FROM QUANTUM KINETIC MONTE CARLO SIMULATIONS"

Absence of Sign Problem in 1D Hubbard Model

In this section we show that there is no sign problem in QKMC simulation of 1D Fermi Hubbard model. We define a propagated state $|\alpha(p)\rangle = |\alpha_\uparrow(p)\alpha_\downarrow(p)\rangle$ along the imaginary-time evolution of state in SSE [1]. Index p means p operators have been applied on an initial electron configuration $|\alpha(0)\rangle$, i.e.,

$$|\alpha(p)\rangle \sim \prod_{i=1}^{p} H_{b_i}|\alpha(0)\rangle \tag{7}$$

We also order the electrons in the state representation so that up-spin creation operators precede the down-spin creation operators. When a diagonal operator, e.g., $n_{i,\sigma} = c^\dagger_{i,\sigma}c_{i,\sigma}$ acts on the propagated state, there is a phase factor $(-1)^{2N^i_\uparrow}$ if $\sigma =\uparrow$ or $(-1)^{2N_\uparrow+2N^i_\downarrow}$ if $\sigma =\downarrow$, where $N^i_{\uparrow,\downarrow}$ is the number of up- or down-spin electrons appearing on lattice site with site index $j < i$, and $N_\uparrow$ is total number of up-spin electrons in the system. In either case, the factor -1 introduced by Fermi statistics always appear twice in the phase factor, leading to a $+1$ phase factor. When an off-diagonal operator acts on the

state, the same phase factors are introduced if OBC is used. Consequently, there is no sign problem in QKMC simulation for 1D Fermi Hubbard model with OBC.

Transition Probabilities in QKMC

In SSE formulation of the partition function expansion [1], there are two kinds of updates: diagonal update and off-diagonal update (loop update). For diagonal update, SSE expansion order goes from n to $n+1$ with transition probability

$$P_j(n \to n+1) = \frac{\beta\langle\alpha(p)|H_b|\alpha(p)\rangle}{N_c - n} \tag{8}$$

and degeneracy $d_j = M_b$ since there are M_b bonds where one diagonal operator can be added. Similarly, SSE expansion order goes from n to $n-1$ with probability

$$P_j(n \to n-1) = \frac{N_c - n + 1}{M_b\beta\langle\alpha(p)|H_b|\alpha(p)\rangle} \tag{9}$$

and degeneracy $d_j = 1$ since it is the only bond we want to remove.

For off-diagonal update, a loop containing N_{Loop} vertices is first constructed according to Ref. [1]. The transition probability for off-diagonal update is then given by

$$P_j = \prod_{i=1}^{N_{Loop}} p_i \tag{10}$$

where p_i is transition probability for the i^{th} vertex [1]. For off-diagonal transition, the degeneracy $d_j = 4N_b$, where N_b is total number of operators in current SSE expansion, since there are $4N_b$ possibilities to pick an entrance leg for constructing the loop.

QKMC for Canonical System

QMC simulation with SSE method is usually carried out in grand canonical systems, where total number of particles can fluctuate. However, if we want to calculate electric current going from the left to the right across the interface in our system (see Fig. 1 in the main text), we should perform QKMC in a canonical system , i.e., by setting $N_L + N_R$ to a fixed value. At half-filling for a 20-site system, for example, $N_L + N_R = 20$.

Diagonal update discussed above keeps the total number of electrons fixed; while off-diagonal update may change the electron number. Off-diagonal transitions that change the total number of electrons in the system will then be rejected.

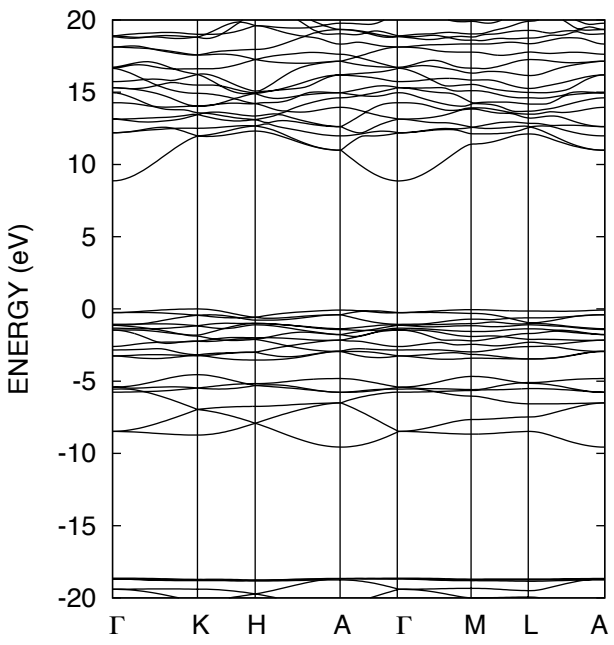

FIG. 6: Electronic band structure for α quartz. Fermi energy is located at 0 eV.

Electronic Band Structure of α Quartz

In this section we describe in detail our calculation of α quartz band structure using Vienna Ab initio Simulation Package (VASP) software package [2, 3]. First principle calculations have been performed within the framework of Density Functional Theory (DFT) to study the band structure of α quartz. The Projector Augmented Wave (PAW) method has been used [4], as implemented in VASP. The plane wave cutoff energy for our calculations is set to 400 eV, and the self-consistent electronic loop is converged to 10^{-5} eV. The Local Density Approximation (LDA) exchange and correlation functional have been used to minimize the total energy. The conjugate gradient algorithm has been used to relax the atomic positions until forces on atoms are smaller than 1 meV/$\mathring{A}$. In order to investigate the electronic structure quantitatively, PBE0 exchange and correlation functional have been used in the ultimate static calculation to correct the eigenlevel structure and the band gap in α quartz.

Figure 6 shows the band structure from our calculation. The indirect gap between valence and conduction bands is around 9 eV in good agreement with other calculated [5] and experimental data [6].

Hopping Integrals from MLWF

Since the electronic band structure was calculated in the previous section, we can proceed to determine the

V (eV)	N_B	t (eV)
0.8	2	0.048
2.36	5	0.116
2.66	8	0.331

TABLE I: Number of Bloch bands N_B involved in the Wannierization process and leading hopping integral t among MLWFs as a function of applied electric potential difference V.

MLWFs for the α quartz system. We first run VASP to generate input files for Wannier90 [7]. The number of Bloch bands N_B to be included in the Wannierization process [8, 9] depends on the applied electric potential difference V. The applied electric field induces holes in the valence bands. An equivalent picture to electron hopping with negative hopping integral is hole hopping with positive hopping integral. This is due to the electron-hole transformation $c^\dagger_{i\sigma} \rightarrow h_{i\sigma}$ and $c_{i,\sigma} \rightarrow h^\dagger_{i,\sigma}$, where $h^\dagger_{i,\sigma}(h_{i\sigma})$ is hole creation (annihilation) operator. Therefore, the kinetic energy part of the Hamiltonian becomes $-tc^\dagger_{i,\sigma}c_{i+1,\sigma} = -th_{i,\sigma}h^\dagger_{i+1,\sigma} = th^\dagger_{i+1,\sigma}h_{i\sigma}$. We should, therefore, look for positive hopping integrals among MLWFs.

Table I lists N_B together with V and the leading positive hopping integral t among MLWFs.

[1] O. F. Syljuasen and A. W. Sandvik, Phys. Rev. E **66**, 046701 (2002).

[2] G. Kresse and J. Furthmuller, Comput. Mat. Sci. **6**, 15 (1996).

[3] G. Kresse and J. Furthmuller, Phys. Rev. B **54**, 11169 (1996).

[4] P. E. Blochl, Phys. Rev. B **50**, 17953 (1994).

[5] J. R. Chelikowsky and M. Schluter, Phys. Rev. B **15**, 4020 (1977).

[6] Z. A. Weinberg, G. W. Rubloff, and E. Bassous, Phys. Rev. B **19**, 3107 (1979).

[7] A. A. Mostofi, J. R. Yates, G. Pizzi, Y. S. Lee, I. Souza, D. Vanderbilt and N. Marzari, Comput. Phys. Commun. **185**, 2309 (2014).

[8] N. Marzari and D. Vanderbilt, Phys. Rev. B **56**, 12847 (1997).

[9] I. Souza, M. Marzari, and D. Vanderbilt, Phys. Rev. B **65**, 035109 (2001).